CD147 and MCT1-Potential Partners in Bladder Cancer Aggressiveness and Cisplatin Resistance

Julieta Afonso,[1,2] Lúcio L. Santos,[3,4] Vera Miranda-Gonçalves,[1,2] António Morais,[5] Teresina Amaro,[6] Adhemar Longatto-Filho,[1,2,7,8] and Fátima Baltazar[1,2]*

[1]*Life and Health Sciences Research Institute (ICVS), School of Health Sciences, University of Minho, Braga, Portugal*
[2]*ICVS/3B's—PT Government Associate Laboratory, Braga/Guimarães, Portugal*
[3]*Department of Surgical Oncology, Portuguese Institute of Oncology (IPO), Porto, Portugal*
[4]*Faculty of Health Sciences, University Fernando Pessoa (UFP), Porto, Portugal*
[5]*Department of Urology, Portuguese Institute of Oncology (IPO), Porto, Portugal*
[6]*Experimental Pathology and Therapeutics Research Center, Portuguese Institute of Oncology (IPO), Porto, Portugal*
[7]*Laboratory of Medical Investigation (LIM 14), Faculty of Medicine, São Paulo State University, São Paulo, Brazil*
[8]*Molecular Oncology Research Center, Barretos Cancer Hospital, São Paulo, Brazil*

The relapsing and progressive nature of bladder tumors, and the heterogeneity in the response to cisplatin-containing regimens, are the major concerns in the care of urothelial bladder carcinoma (UBC) patients. The metabolic adaptations that alter the tumor microenvironment and thus contribute to chemoresistance have been poorly explored in UBC setting. We found significant associations between the immunoexpressions of the microenvironment-related molecules CD147, monocarboxylate transporters (MCTs) 1 and 4, CD44 and CAIX in tumor tissue sections from 114 UBC patients. The presence of MCT1 and/or MCT4 expressions was significantly associated with unfavorable clinicopathological parameters. The incidence of CD147 positive staining significantly increased with advancing stage, grade and type of lesion, and occurrence of lymphovascular invasion. Similar associations were observed when considering the concurrent expression of CD147 and MCT1. This expression profile lowered significantly the 5-year disease-free and overall survival rates. Moreover, when selecting patients who received platinum-based chemotherapy, the prognosis was significantly worse for those with MCT1 and CD147 positive tumors. CD147 specific silencing by small interfering RNAs (siRNAs) in UBC cells was accompanied by a decrease in MCT1 and MCT4 expressions and, importantly, an increase in chemosensitivity to cisplatin. Our results provide novel insights for the involvement of CD147 and MCTs in bladder cancer progression and resistance to cisplatin-based chemotherapy. We consider that the possible cooperative role of CD147 and MCT1 in determining cisplatin resistance should be further explored as a potential theranostics biomarker.

Key words: CD147; chemoresistance; monocarboxylate transporters; tumor microenvironment; urothelial bladder cancer

INTRODUCTION

Urothelial bladder carcinoma (UBC), the most frequent type (90%) of bladder cancer and the second most common urogenital malignancy, is a complex disease with variable natural history and clinical behavior. The majority of the tumors are non-muscle invasive (NMI) low-grade papillary lesions characterized by frequent recurrences; the remaining display a phenotype of muscle-invasive (MI) tumors. An intermediate sub-variant of high-grade NMI tumors harbors an enhanced risk of progression [1]. Due to the high propensity of dissemination, MI tumors are generally treated by radical cystectomy (RC), pelvic lymphadenectomy and/or perioperative cisplatin-containing chemotherapy [2]. However, chemotherapy responses are very heterogeneous and frequently impaired by resistance [3].

CD147 (or EMMPRIN, extracellular matrix metalloproteinase inducer) is a transmembrane protein member of the immunoglobulin superfamily of receptors. Originally identified as a matrix metalloproteinase (MMP) inducer, CD147 also promotes angiogenesis, migration and invasion [4]. Importantly,

Abbreviations: ABC, ATP-binding cassette; AJCC, American Joint Committee on Cancer; bp, base pairs; CA, carbonic anhydrase; CDDP, cis-diamminedichloroplatinum(II); CIS, carcinoma in situ; DFS, disease-free survival; EGFR, epidermal growth factor receptor; EMMPRIN, extracellular matrix metalloproteinase inducer; FBS, fetal bovine serum; H&E, hematoxylin–eosin; HIF, hypoxia-inducible factor; LVI, lymphovascular invasion; MAPK, mitogen-activated protein kinase; MCTs, monocarboxylate transporters; MDR1, multidrug resistance protein 1; MI, muscle invasive; MMP, matrix metalloproteinase; MRP-1, multi-drug resistance-associated protein-1; nM, nanomolar; NMI, non-muscle invasive; OS, overall survival; PI, propidium iodide; PI3K, phosphatidylinositol 3-kinase; RC, radical cystectomy; rpm, rotations per minute; RT-PCR, reverse transcription polymerase chain reaction; siRNA, small interfering ribonucleic acid; TUR, transurethral resection; UBC, urothelial bladder carcinoma; μg, microgram; μm, micrometer; VEGF, vascular endothelial growth factor; WHO, World Health Organization.

Conflicts of interest: The authors declare that they have no conflict of interest to disclose.

Grant sponsor: Life and Health Sciences Research Institute (ICVS); Grant sponsor: Portuguese Science and Technology Foundation (FCT); Grant number: SFRH/BD/51997/2012

*Correspondence to: Life and Health Sciences Research Institute (ICVS), School of Health Sciences, University of Minho, Campus de Gualtar, 4710-057 Braga, Portugal.

Received 6 November 2013; Revised 4 July 2014; Accepted 5 August 2014

DOI 10.1002/mc.22222

Published online in Wiley Online Library (wileyonlinelibrary.com).

CD147, through hyaluronan-CD44 interaction, cross-talks with various multi-drug transporters of the ABC (ATP-binding cassette) family classically associated with anti-apoptotic signaling and chemotherapy resistance [5]. Moreover, these constitutive interactions contribute to the regulation of monocarboxylate transporter localization and function at the plasma membrane [6].

Monocarboxylate transporters (MCTs) comprise fourteen members that share the same basic structure, although only the membrane-bound proton-coupled isoforms—MCT1, MCT2, MCT3, and MCT4–transport monocarboxylates, namely lactate, through the plasma membrane [7]. The efflux of lactate from the malignant cells to the tumor microenvironment is crucial to maintain metabolic homeostasis. The malignant cells usually display high glycolytic rates even under aerobic conditions, a phenomenon known as the "Warburg effect" [8]. Hypoxia, a constitutive trait of tumors, is considered to be a trigger mechanism of the glycolytic phenotype [9]. Under hypoxic stress, hypoxia-inducible factor (HIF)-1α amplifies an adaptive response that promotes glycolysis and induces the expression of pH regulators, such as carbonic anhydrase IX (CAIX) and MCTs, to assure intracellular pH balance. The high amounts of lactate extruded from the malignant cells, mainly through MCT1 and MCT4, contribute to acidification of the tumor microenvironment, supporting increased migration and invasion abilities of the primary tumor [10].

The preponderance of the tumor microenvironment in UBC setting has been poorly explored. A few studies have reported upregulation of microenvironment-related molecules, namely CD147 [11–13], CD44 [14], CAIX [15], and MCT4 [16], and their significant impact on the prognosis of the patients. Als et al. [12] demonstrated that CD147 positivity was able to predict response and survival following cisplatin-containing chemotherapy in patients with advanced UBC. In other types of malignancies, increasing evidence suggest that the upregulation of the aforementioned molecules contributes to a hyper-glycolytic acid-resistant microenvironment that favors tumor growth, invasion and metastasis, suppresses host immune defences, and impairs chemotherapy response [17–19].

In order to elucidate the role of microenvironment-related molecules in UBC, namely their impact on chemoresistance, we aimed to assess, in 114 UBC patients, the clinical and prognostic significance of MCT1, MCT4, CD147, CD44, and CAIX expressions. Additionally, we intended to characterize the chemosensitivity of parental and CD147-silenced UBC cell lines to cisplatin.

MATERIALS AND METHODS

Patients and Tissue Samples

Representative formalin-fixed paraffin-embedded surgical specimens were obtained from 114 patients with urothelial bladder carcinomas who underwent transurethral resection (TUR) and/or radical cystectomy (RC) at the Portuguese Institute of Oncology, Porto, from January 1996 to May 2006. In our cohort, we did not include patients diagnosed with urothelial carcinomas with variant histology, squamous cell or adenocarcinomas, patients who had an insufficient follow-up time and/or patients whose tumor samples were inadequate for further study. Prior approval was obtained from the Ethics Committee of the Portuguese Institute of Oncology. The median age of the patients was 70 yr (range 41–86); ninety-four (82.5%) were male and twenty (17.5%) were female. Additionally, tissue sections were obtained from normal-like areas of the urinary bladder of six autopsy patients without history of bladder cancer.

Each surgical product was examined according to the guidelines of the College of American Pathologists [20]. Hematoxylin–eosin (H&E)-stained sections were reviewed according to standard histopathological examination by two independent pathologists. Lesions were classified according to the American Joint Committee on Cancer (AJCC) [21] and to the World Health Organization (WHO) [22] classification systems. For statistical analysis, tumors were divided into three groups based on T stage.

Forty-two (36.8%) patients underwent TUR with curative intention; 22 of these patients were treated by RC following disease recurrence and progression or when multiple carcinoma in situ (CIS) lesions were observed in the pathological specimen. Seventy-two (63.2%) patients had RC as their first treatment. Platinum-based chemotherapy regimens were administered to 31 (27.2%) patients (neoadjuvant: six patients, adjuvant: nine patients, palliative: 16 patients). Twenty-seven (23.7%) patients presented loco-regional metastases at the time of RC. Mean and median follow-up were 38.2 and 37.0 months (range 1–132), respectively. Recurrence was defined as the reappearance of UBC (loco-regional dissemination or distant metastasis) more than three months after TUR/RC, occurring in 74 (64.9%) patients. Disease-free survival (DFS) was defined as the time from the TUR/RC until recurrence. Overall survival (OS) was defined as the time from the TUR/RC until death by bladder cancer or the last clinical assessment.

Cell Lines and General Cell Culture Procedures

In the present study, four urothelial bladder carcinoma cell lines were used. As we intended to characterize the chemosensitivity of the cell lines to cisplatin (the platinum compound usually administered to patients with muscle-invasive tumors), we selected a NMI-UBC cell line (5637) and three MI-UBC cell lines (T24, MCR, and HT1376). T24 was obtained from Leibniz Institute DSMZ—German Collection of Microorganisms and Cell Cultures; 5637, MCR and HT1376 were kindly provided by Professor Paula

Videira, Universidade Nova de Lisboa, Lisboa, Portugal. Cell line authentication was performed by Pinto-Leite et al. [23]; genotyping confirmed their complete identity. The cell lines were cultured as a monolayer in RPMI Medium 1640 (Gibco®) supplemented with antibiotics (1% penicillin/streptomycin solution, Gibco®) and 10% fetal bovine serum (FBS, Gibco®). Cells were incubated in a humidified atmosphere at 37°C and 5% CO_2, and were routinely subcultured by trypsinization.

Immunohistochemistry and Immunocytochemistry

Representative 4-μm-thick UBC sections were stained by immunohistochemistry, according to the streptavidin-biotin-peroxidase complex technique (Ultravision Detection System Anti-polyvalent, HRP, Lab Vision Corporation, Waltham, MA) for MCT4, CD147, CD44, and CAIX detection, and to the avidin–biotin–peroxidase complex assay (VECTASTAIN Elite ABC Reagent, RTU, Vector Laboratories, Burlingame, CA) for MCT1 detection, as previously described [13,24,25]. The primary antibodies were obtained from Chemicon® (MCT1, AB3538P), Santa Cruz Biotechnology® (MCT4, H-90, sc-50329), Zymed® (CD147, 18–7344), AbD Serotec (CD44, MCA2726) and AbCam (CAIX, ab15086). These antibodies were used in 1:200 dilution (MCT1), 1:500 dilution (MCT4 and CD147), 1:1000 dilution (CD44) and 1:2000 dilution (CAIX), and incubated on the sections for 2 h (MCT4, CD147, CD44, CAIX) or overnight (MCT1), at room temperature. Negative controls were carried out by replacing the primary antibodies with a universal negative control antibody (N1699, Dako, Glostrup, Denmark). Colon carcinoma and gastric carcinoma sections were used as positive controls for MCT1, MCT4, CD147 and CD44 detection, and for CAIX detection, respectively.

The immunocytochemistry procedure for detecting MCT1, MCT4, and CD147 expression in the UBC cell lines was performed in 4 μm-thick cytoblock sections, following the protocol mentioned for UBC sections, as described above. The paraffin cytoblocks were made from concentrated cell suspensions by centrifuging fresh cell suspensions at 1200 rpm for 5 min. Cell pellets were incubated overnight with formaldehyde 3.7%, re-centrifuged, processed in an automatic tissue processor (TP1020, Leica, Nussloch, Germany), and then included into paraffin (block-forming unit EG1140H, Leica).

Evaluation of Immunohistochemistry and Immunocytochemistry Results

The immunostained tissue sections were evaluated by light microscopy for cytoplasmic and/or plasma membrane staining by two independent observers. Discordant cases were re-evaluated and classified by consensus. The grading system used was semi-quantitative [13,24–25], considering the sum of the percentage of immunoreactive cells (0, 0% of positive cells; 1, <5% of positive cells; 2, 5–50% positive cells; score 3, >50% of positive cells) and the intensity of staining (0, negative; 1, weak; 2, intermediate; 3, strong); final scores ≥4 were considered positive for all of the biomarkers studied. Finally, the plasma membrane positive cases were analyzed separately.

The expression of the biomarkers on the cytoblocks sections was also assessed, distinguishing between cytoplasmic and plasma membrane staining.

Downregulation of CD147 Expression

Silencing of CD147 expression in MCR and HT1376 cell lines was accomplished by reverse transfection of 50 nM siRNA (siRNA for CD147, SASI_Hs01_00156882, Sigma–Aldrich®; St. Louis, MO, control scramble siRNA, 4390843, Ambion®); lipofectamine (13778-075, Invitrogen™) was used as permeabilization agent, following the manufacturer's instructions. Cells were transfected once and collected on days 5 and 8 after transfection. Specific silencing of the targeted gene was confirmed by Western blotting and reverse transcription polymerase chain reaction (RT–PCR) analysis.

Western Blotting

Parental UBC cell lines grown to 80% confluence, and siRNA cells grown until days 5 and 8 after transfection, were scraped in cold PBS and then homogenized in lysis buffer (supplemented with protease inhibitors) for 10 min. Cell lysates were collected after centrifugation at 13,000 rpm, 15 min at 4°C. The Bio-Rad Dc Protein Assay (500-0113, Bio-Rad, Hercules, CA) was used for protein quantification. Equal amounts (20 μg) of total protein were separated on 10% polyacrylamide gel by SDS–PAGE and transblotted onto nitrocellulose membranes (Amersham Biosciences) in 25 mM Tris-base/glycine buffer. MCT1, MCT4 and CD147 expressions were evaluated by incubating the membranes overnight at 4°C with specific primary polyclonal antibodies against MCT1 (1:200 dilution, H-1, sc-365501, Santa Cruz Biotechnology®), MCT4 (1:2000 dilution, H-90, sc-50329, Santa Cruz Biotechnology®) and CD147 (1:200 dilution, sc-71038, Santa Cruz Biotechnology®). β-Actin (1:300 dilution, I19, sc-1616, Santa Cruz Biotechnology®) was used as loading control. Blots were developed with enhanced chemiluminescence (Supersignal West Femto kit, 34096, Pierce, Waltham, MA) using anti-mouse or anti-goat Ig secondary antibodies coupled to horseradish peroxidase. Band densitometry analysis with the Image J software (version 1.41, National Institutes of Health) was performed for quantification of Western blot results.

RT-PCR Assay

Total cellular RNA was extracted using TRIzol reagent (15596-026, Ambion®, Austin, TX) and their concentration determined spectrophotometrically in a Nanodrop 2000 (Thermo Scientific Inc., Waltham,

MA). 1 μg RNA was reverse-transcribed using a high capacity cDNA reverse transcription Kit (4368814, Applied Biosystems®, Carlsbad, CA), according to the manufacturer's instructions. The primer sequences used were for CD147 RT-PCR were (sense) 5′-CCATGCTGGTCTGCAAGTCAG-3′ and (antisense) 5′-CCGTTCATGAGGGCCTTGTC-3′, and to β-actin RT-PCR were (sense) 5′-CTGGAACGGTGAAGGTGACA-3′ and (antisense) 5′-AAGGGACTTCCTGTAACAACGCA-3′. Primer annealing occurred at 55°C for 30 s during 30 cycles for CD147, and at 56°C for 30 s during 35 cycles for β-actin. The PCR products were analyzed on a 2% agarose gel containing ethidium bromide.

Cell Viability Assay

To assess the chemosensitivity of the UBC cell lines to cisplatin (CDDP, *cis*-diamminedichloroplatinum-[II])s, cells were seeded in triplicate into 48-well plates at different densities, based on the growth characteristics of each cell line (1.2×10^4 T24 and 5637 cells per well, 1.5×10^4 HT1376 cells per well, 2×10^4 MCR and siRNA-HT1376 cells per well and 3×10^4 siRNA–MCR cells per well), and incubated for 2 (non-siRNA cell lines) or 5 (siRNA cell lines) days. The medium was then removed and replaced with fresh medium containing CDDP with varying concentrations (1–100 μg/ml). Stock solutions of 1 mg/ml CDDP in 10% NaCl were kindly provided by the Pharmaceutical Services of the Portuguese Institute of Oncology, Porto, Portugal, from which the working solutions were prepared. The effect of the treatment with CDDP on cell viability was determined at 72 h by the MTS (3-(4,5-dimethylthiazol-2-yl)-5-(3-carboxymethoxyphenyl)-2-(4-sulfophenyl)-2H-tetra-zolium) assay (G3580, Promega, Madison, WI) according to the manufacturer's instructions. The IC50 values (CDDP concentration that corresponds to 50% of cell growth inhibition) were estimated from at least three independent experiments, using GraphPad Prism 5 Software.

Cell Cycle Analysis

Cells were seeded in 6-well plates at different densities (5×10^5 T24 and 5637, 8×10^5 HT1376 and 1×10^6 MCR cells per well). After 42 h of incubation, the cells were starved in FBS-free medium during 6 h, and then treated with the specific CDDP IC_{50} dose during 72 h. Cells were trypsinized and fixed in 70% ethanol (30 min at 4°C), followed by staining with propidium iodide (PI) solution (20 μg/ml of PI [81845, Sigma] + 250 μg/ml of RNAse [12091-021, Invitrogen™] diluted in 0.01% Triton X-100 in PBS) at 50°C during 50 min. PI stained cells were analyzed by flow cytometry (LSRII model, BD Biosciences, San Jose, CA), considering a total of 15.000 events, and the cell cycle distribution was determined with the FlowJo software (version 7.6, Tree Star, Inc, Ashland, OR). The assay was repeated at least three times.

Cell Death Assay

Cell death rate was determined by the Annexin-V-FLOUS staining Kit (Roche Diagnostics). Cells were seeded in 6-well plates at different densities (5×10^5 T24 and 5637, 8×10^5 HT1376 and 1×10^6 MCR cells per well). After 48 h of incubation, cells were treated with the specific CDDP IC_{50} dose during 72 h, followed by collection and staining with annexin V/PI, according to the manufacturer's instructions (15 min of incubation in the staining solutions, at room temperature). The percentage of cell death was assessed by flow cytometry (LSRII model, BD Biosciences), considering a total of 20,000 events, and the results were analyzed using the FlowJo software (version 7.6, Tree Star, Inc). The assay was repeated at least three times.

Statistical Analysis

The immunohistochemistry results were analyzed using the Statistical Package for Social Sciences (SPSS) software for Windows, version 18.0. Associations between the immunoexpression of the biomarkers and the clinicopathological parameters were examined for statistical significance using Pearson's chi-square (χ^2) test and Fisher's exact test (when $n < 5$). Five-year DFS and OS rates were evaluated using Kaplan–Meier curves and differences were analyzed by Log-Rank or Breslow tests. *P* values lower than 0.05 were considered significant. Variables that achieved statistical significance in the univariate analysis were entered in a multivariate analysis using Cox proportional hazards analysis.

The results of the in vitro studies were analyzed using the GraphPad Prism 5 software, with the Student's *t*-test, considering significant *P* values lower than 0.05.

RESULTS

Characterization of MCT1, MCT4, CD147, CD44 and CAIX Expressions in Urothelial Bladder Tumors

Prognostic significance of the clinicopathological parameters

The 5-year DFS and OS rates were significantly influenced by T3/T4 pathologic stage ($P < 0.001$), muscle-invasive type of lesion ($P < 0.001$), occurrence of lymphovascular invasion (DFS, $P = 0.002$; OS, $P < 0.001$) and presence of loco-regional metastases (DFS, $P = 0.007$, OS, $P < 0.001$) (data not shown).

Immunoexpression of the biological parameters

A total of 114 UBC samples and six non-neoplastic bladder samples were analyzed for MCT1, MCT4, CD147, CD44, and CAIX expressions. After testing different grading systems considering the semi-quantitative evaluation of extension and intensity of staining (cytoplasmic expression, with or without plasma membrane staining), we adopted the final

immunoreaction score ≥4 as the more suitable for explaining the results obtained with all of the studied biomarkers, as described by others [26]. Due to the membrane localization of the biomarkers, plasma membrane staining was additionally assessed separately.

Regarding MCT1 and MCT4 immunoexpressions (Figure 1A-i and ii, respectively), 36 (31.6%) and 50 (43.9%) UBC cases were scored positive, respectively; plasma membrane staining was observed in 44 (38.6%) and 64 (56.1%) cases, respectively. Stromal and endothelial cells were negative for both biomarkers, and served as internal negative controls. None of the normal bladder samples expressed MCT1; two non-neoplastic sections showed cytoplasmic staining for MCT4, but the plasma membrane was negative in the six observed sections.

When considering the expression of the chaperones CD147 and CD44 (Figure 1A iii, iv and v, respectively), the majority of the tumor tissues was positive both for global immunoreaction [CD147: 68 (59.6%); CD44: 57 (50.0%)] and plasma membrane staining (CD147: 70 [61.4%]; CD44: 77 [67.5%]). The stroma was negative for CD147 immunoreaction in all of the cases (Figure 1A-iii); however, although CD44 positive tumors presented negative stromas (Figure 1A-iv), CD44 negative tumors had their stromal cells stained (Figure 1A-v). Regarding the non-neoplastic bladder samples, the majority was negative for CD147 staining, while no difference was observed when evaluating CD44 expression.

CAIX positive immunoexpression (Figure 1A-vi) was observed in the vast majority of the UBC samples (global immunoreaction: 72 [63.2%]; plasma membrane staining: 92 [80.7%]); plasma membrane positive cases exhibited a heterogeneous pattern, with the luminal face of NMI papillary lesions and the centre of MI lesions presenting a strong intensity of staining. None of the normal bladders expressed CAIX.

Associations among the biological parameters

Significant associations were found between the expression of MTCs, CD147, and CD44 in the tumor samples (Table 1). CD147 and CD44 immunoreaction was also correlated: 70.2% (40/57) and 67.5% (52/77) of the positive sections for CD44 (global expression and plasma membrane staining, respectively) expressed CD147 ($P = 0.035$ and $P = 0.065$, respectively; data not shown). Additionally, significant associations were found when comparing immunoreactive samples for MCT4 (92%, 46/50, $P = 0.007$), CD147 (86.9%, 59/68, $P = 0.046$) and CD44 (89.5%, 51/57, $P = 0.018$) with CAIX plasma membrane positive cases (data not shown).

Clinical and prognostic significance of the biological parameters

The presence of MCT1 and/or MCT4 global immunoexpression, and MCT1 plasma membrane staining, was significantly associated with unfavourable clinico-pathological parameters, such as increasing stage, MI type of lesion and occurrence of lymphovascular invasion (Table 2). MCT1 expression (global immunoreaction) had a negative influence on 5-year DFS ($P = 0.053$) and OS ($P = 0.065$) rates (Figure 1B).

Regarding CD147 expression, 80.0% of pT3/pT4 tumors, 75.0% of MI tumors and 84.6% of the tumors with LVI occurrence were positive for CD147 global immunoexpression (Table 2). This expression profile lowered significantly the 5-year DFS ($P = 0.027$) and OS ($P = 0.018$) rates (Figure 1B).

In order to assess the clinical and prognostic significance of the combined analysis of MCT1 and CD147 immunoreaction, we considered two groups: group 1, including cases with 0 or 1 positive biomarkers, and group 2, including cases with two positive biomarkers. Group 2 had unfavorable clinico-pathological parameters—72.7% (24/33, $P < 0.001$), 90.9% (30/33, $P < 0.001$), and 60.6% (20/33, $P < 0.001$) of the MCT1 and CD147 positive cases were pT3/pT4, MI and with LVI occurrence tumors, respectively (data not shown)—and a lower 5-year DFS ($P = 0.033$) and OS ($P = 0.037$) (data not shown). Notably, when selecting the patients who received platinum-based chemotherapy ($n = 31$), the prognosis was significantly worse for group 2 ($n = 11$)—patients with 0 or 1 positive biomarkers had median DFS and OS times of 25.8 (95% CI 20.4–31.2) and 42.2 (95% CI 33.9–50.4) months, respectively, which were reduced to 11.7 (95% CI 6.7–16.2) and 12.4 (95% CI 1.0–32.5) months, respectively, if the tumors were MCT1 and CD147 positive ($P = 0.072$ and 0.026, respectively; Figure 1B).

CD44 plasma membrane positivity was predominant in pT3/pT4 and MI UBC samples. Conversely, the majority of high-grade papillary lesions were CAIX positive. Regarding the global immunoreaction for CAIX, 87.5% of high-grade papillary tumors, 69.3% of the tumors without LVI occurrence and 67.8% of the cases without loco-regional metastasis were scored positive (Table 2).

The aforementioned associations were found when analyzing a series of 114 UBC patients, which includes six patients that received neo-adjuvant platinum-based chemotherapy regimens. Since this could introduce a bias variable, the statistical analysis was also performed without those six cases; however, no differences were observed, and we decided to include the cases in the final results.

Multivariate Analysis

The parameters that significantly influenced the 5-year DFS and OS rates were entered in the multivariate analysis model. None of the aforementioned variables was identified as an independent prognostic factor.

Immunoexpression of MCT1, MCT4 and CD147 in Urothelial Bladder Cancer Cell Lines

All UBC cell lines expressed MCT1, MCT4, and CD147, as detected by Western blot (Figure 2A) and immunocytochemistry (Figure 2B). MCT4 and CD147 were expressed predominantly at the plasma membrane. In T24 cell line, MCT1 expression was membranous, while in the remaining cell lines, both plasma membrane and cytoplasm were stained.

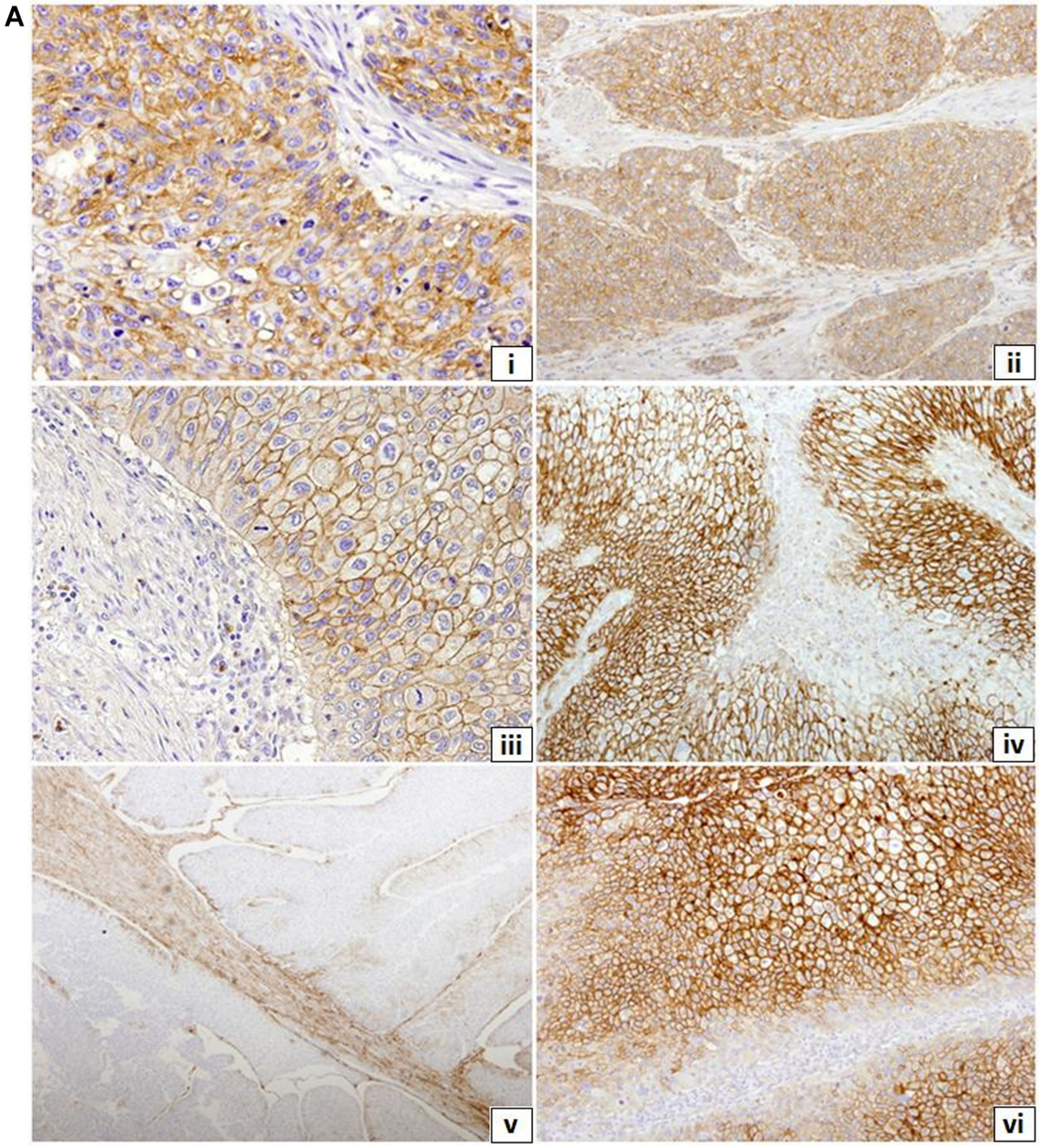

Figure 1. Immunohistochemical positive reactions (A) for MCT1 (i, ×200 amplification), MCT4 (ii, ×100 amplification), CD147 (iii, ×200 amplification), CD44 (iv, ×100 amplification; v, ×40 amplification) and CAIX (vi, ×100 amplification) in urothelial bladder carcinoma cells, and influence of selected biomarkers on survival rates (B). A, ii to iv, muscle-invasive tumors exhibiting cytoplasmic and membrane immunoexpression of the selected biomarkers in the malignant urothelium, with negative stromas; v, a non-muscle invasive tumor showing an inverted CD44 staining pattern, with negative malignant cells and positive stroma; vi, a muscle-invasive tumor stained for CAIX in the plasma membrane of the malignant urothelial cells, where the tumor core is significantly more intensely stained than the invasive front. B, Kaplan–Meier curves demonstrating 5-year disease-free survival and overall survival rates based on MCT1 or CD147 immunoexpression status in bladder tumor sections ($n = 114$), and on MCT1 and CD147 concomitant immunoexpression in selected platinum-treated patients ($n = 31$). Log-Rank or Breslow tests were used to determine P values.

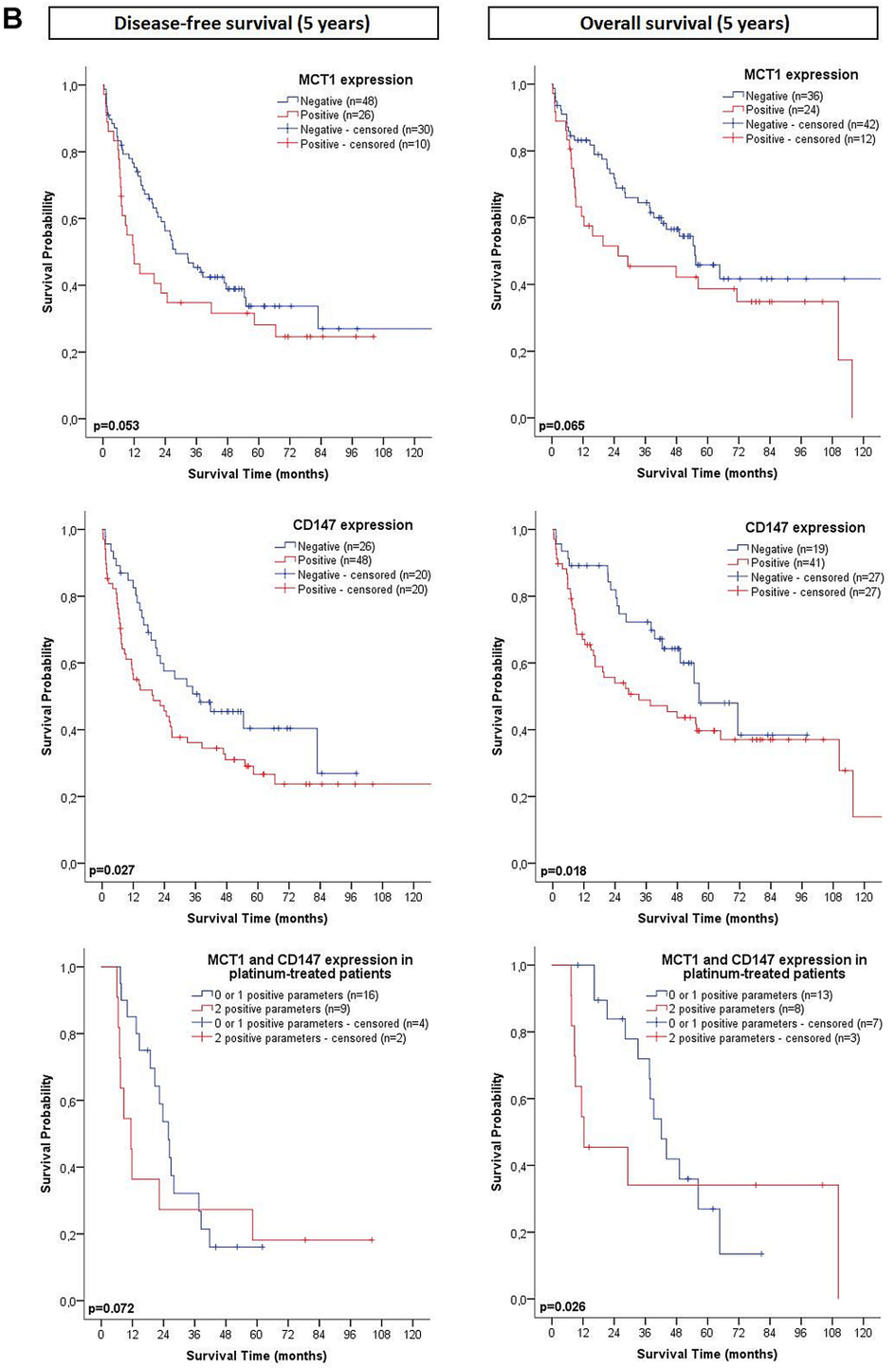

Figure 1. (*Continued*)

Table 1. Association Between MCTs, and CD147 and CD44 Global Immunoreaction (Cytoplasmic Expression, With or Without Plasma Membrane Staining) or Plasma Membrane Immunoexpression

		CD147			CD44		
	n	Negative (%)	Positive (%)	P^a	Negative (%)	Positive (%)	P^a
MCT1							
Global immunoreaction							
Negative (%)	78	43 (55.1)	35 (44.9)	<0.001	46 (59.0)	32 (41.0)	0.008
Positive (%)	36	3 (8.3)	33 (91.7)		11 (30.6)	25 (69.4)	
Plasma membrane							
Negative (%)	70	34 (48.6)	36 (51.4)	0.006	26 (37.1)	44 (62.9)	0.220
Positive (%)	44	10 (22.7)	34 (77.3)		11 (25.0)	33 (75.0)	
MCT4							
Global immunoreaction							
Negative (%)	64	41 (64.1)	23 (35.9)	<0.001	40 (62.5)	24 (37.5)	0.004
Positive (%)	50	5 (10.0)	45 (90.0)		17 (34.0)	33 (66.0)	
Plasma membrane							
Negative (%)	50	26 (52.0)	24 (48.0)	0.012	21 (42.0)	29 (58.0)	0.070
Positive (%)	64	18 (28.1)	46 (71.9)		16 (25.0)	48 (75.0)	

[a] χ^2 or Fisher's exact tests.

In Vitro Effect of CDDP in Urothelial Bladder Cancer Cell Lines

In order to characterize the response of four different parental UBC cell lines to CDDP, IC_{50} values were estimated after 72 h of treatment (Figure 3A) (previous protocol optimization, with incubation periods of 24, 48 and 72 h, was done). We observed that 5637 and T24 cell lines present a gradual decrease in total biomass in a CDDP dose-dependent manner. HT1376 and MCR cell lines were less sensitive to CDDP effect: at the initial concentrations, only a slight decrease on cell viability was noted. To further elucidate CDDP effect on cell cycle distribution (Figure 3B) and cell death (Figure 3C), the UBC cell lines were treated with the CDDP IC_{50} predetermined doses. 5637, T24, and HT1376 cell lines presented a decrease in G1 phase and an increase in S + subG1 phase's cell populations (differences statistically significant for T24 and HT1376). The drug induced cell death in 5637 and T24 cell lines: we observed a marked increase in late apoptotic/necrotic cell populations (differences statistically significant for 5637). Regarding the cell cycle distribution of MCR cell line, we observed a significant decrease in G1 and an arrest in S + G2 phase's cell populations. We confirmed this cytostatic action of the drug in MCR cells through the cell death assay.

Effect of CD147 Downregulation on Urothelial Bladder Cancer Cells' Biology and Response to CDDP Treatment

The characterization of the effect of CDDP treatment on cell viability, cell cycle distribution and cell death, allowed us to choose two of the cell lines for subsequent downregulation studies. HT1376 and MCR cells seem to be less sensitive to CDDP effect. Based on this, we used specific siRNA targeting CD147 mRNA to downregulate CD147. By Western blotting, we confirmed a marked decrease in CD147 expression in both cell lines, most notably following 6 and 10 days after reverse transfection; the transfection with scramble siRNA did not alter protein expression. Once the protocol has been optimized, we proceeded with CDDP treatment in siRNA-HT1376 and siRNA-MCR cells. Since we had previously determined CDDP IC_{50} values for the parental cell lines after 72 h of exposure to the drug, we followed the same procedure with the siRNA cell lines, by treating the cells between days 5 and 8 after reverse transfection. However, we were only able to continue the experiment with HT1376 cell line, since MCR cells became non-viable after transfection plus CDDP treatment (confirmed in repeated assays). CD147 silencing at days 5 and 8 after transfection was confirmed by Western blot and RT-PCR (Figure 4A and B); the decrease in CD147 expression was accompanied by a decrease in MCT1 and MCT4 expressions (Figure 4A). IC_{50} values were determined (Figure 4C), which allowed us to conclude that siCD147-HT1376 cells were more sensitive to CDDP treatment than siScramble-HT1376 cells (the disparity between IC_{50} values for parental HT1376 and siScramble-HT1376 cells is due to the different number of cells plated per well).

DISCUSSION

Radical cystectomy with bilateral lymphadenectomy provides a cure for most of the UBC patients with muscle-invasive organ-confined lesions [2], but regional lymph node and visceral metastases are frequently found; in these cases, perioperative chemotherapy in fit patients is mandatory. Multi-drug platinum-based regimens provide the best response rates. Cisplatin is the main component of the MVAC

Table 2. Association Between MCT1, MCT4, CD147, CD44 and CAIX Global Immunoreaction (Cytoplasmic Expression, With or Without Plasma Membrane Staining) or Plasma Membrane Staining, and the Clinicopathological Parameters

		MCT1			MCT4			CD147			CD44			CAIX		
Clinicopathological parameter	*n*	Negative (%)	Positive (%)	*P*[a]	Negative (%)	Positive (%)	*P*[a]	Negative (%)	Positive (%)	*P*[a]	Negative (%)	Positive (%)	*P*[a]	Negative (%)	Positive (%)	*P*[a]
Global immunoreaction																
Stage																
pTa, pT1, pTis	46	42 (91.3)	4 (8.7)	<0.001	33 (71.7)	13 (28.3)	0.022	29 (63.0)	17 (37.0)	<0.001	27 (58.7)	19 (41.3)	0.076	13 (28.3)	33 (71.7)	0.187
pT2	18	12 (66.7)	6 (33.3)		8 (44.4)	10 (55.6)		7 (38.9)	11 (61.1)		11 (61.1)	7 (38.9)		6 (33.3)	12 (66.7)	
pT3, pT4	50	24 (48.0)	26 (52.0)		23 (46.0)	27 (54.0)		10 (20.0)	40 (80.0)		19 (38.0)	31 (62.0)		23 (46.0)	27 (54.0)	
Grade and Type of lesion																
NMIP UC, low grade	10	9 (90.0)	1 (10.0)	<0.001	8 (80.0)	2 (20.0)	0.021	9 (90.0)	1 (10.0)	<0.001	6 (60.0)	4 (40.0)	0.417	5 (50.0)	5 (50.0)	0.001
NMIP UC, high grade	32	30 (93.8)	2 (6.2)		21 (65.6)	11 (34.4)		18 (56.2)	14 (43.8)		18 (56.2)	14 (43.8)		4 (12.5)	28 (87.5)	
NMI UC in situ	4	3 (75.0)	1 (25.0)		4 (100.0)	0 (0.0)		2 (50.0)	2 (50.0)		3 (75.0)	1 (25.0)		4 (100.0)	0 (0.0)	
MI UC	68	36 (52.9)	32 (47.1)		31 (45.6)	37 (54.4)		17 (25.0)	51 (75.0)		30 (44.1)	38 (55.9)		29 (42.6)	39 (57.4)	
Lymphovascular invasion																
Negative	75	59 (78.7)	16 (21.3)	0.002	48 (64.0)	27 (36.0)	0.028	40 (53.3)	35 (46.7)	<0.001	39 (52.0)	36 (48.0)	0.693	23 (30.7)	52 (69.3)	0.068
Positive	39	19 (48.7)	20 (51.3)		16 (41.0)	23 (59.0)		6 (15.4)	33 (84.6)		18 (46.2)	21 (53.8)		19 (48.7)	20 (51.3)	
Loco-regional metastasis																
Negative	87	60 (69.0)	27 (31.0)	0.817	49 (56.3)	38 (43.7)	1.000	38 (43.7)	49 (56.3)	0.262	44 (50.6)	43 (49.4)	1.000	28 (32.2)	59 (67.8)	0.064
Positive	27	18 (66.7)	9 (33.3)		15 (55.6)	12 (44.4)		8 (29.6)	19 (70.4)		13 (48.1)	14 (51.9)		14 (51.9)	13 (48.1)	
Plasma membrane staining																
Stage																
pTa, pT1, pTis	46	37 (80.4)	9 (19.6)	0.003	23 (50.0)	23 (50.0)	0.453	19 (41.3)	27 (58.7)	0.654	21 (45.7)	25 (54.3)	0.013	8 (17.4)	38 (82.6)	0.609
pT2	18	9 (50.0)	9 (50.0)		6 (33.3)	12 (66.7)		8 (44.4)	10 (55.6)		7 (38.9)	11 (61.1)		5 (27.8)	13 (72.2)	
pT3, pT4	50	24 (48.0)	26 (52.0)		21 (42.0)	29 (58.0)		17 (34.0)	33 (66.0)		9 (18.0)	41 (82.0)		9 (18.0)	41 (82.0)	
Grade and Type of lesion																
NMIP UC, low grade	10	9 (90.0)	1 (10.0)	0.006	5 (50.0)	5 (50.0)	0.758	5 (50.0)	5 (50.0)	0.052	3 (30.0)	7 (70.0)	0.032	2 (20.0)	8 (80.0)	<0.001
NMIP UC, high grade	32	25 (78.1)	7 (21.9)		16 (50.0)	16 (50.0)		10 (50.0)	22 (68.8)		15 (46.9)	17 (53.1)		2 (6.2)	30 (93.8)	
NMI UC in situ	4	3 (75.0)	1 (25.0)		2 (50.0)	2 (50.0)		4 (100.0)	0 (0.0)		3 (75.0)	1 (25.0)		4 (100.0)	0 (0.0)	
MI UC	68	33 (48.5)	35 (51.5)		27 (39.7)	41 (60.3)		25 (36.8)	43 (63.2)		16 (23.5)	52 (76.5)		14 (20.6)	54 (79.4)	
Lymphovascular invasion																
Negative	75	52 (69.3)	23 (30.7)	0.025	37 (49.3)	38 (50.7)	0.115	33 (44.0)	42 (56.0)	0.110	28 (37.3)	47 (62.7)	0.144	15 (20.0)	60 (80.0)	1.000
Positive	39	18 (46.2)	21 (53.8)		13 (33.3)	26 (66.7)		11 (28.2)	28 (71.8)		9 (23.1)	30 (76.9)		7 (17.9)	32 (82.1)	
Loco-regional metastasis																
Negative	87	52 (59.8)	35 (40.2)	0.652	37 (42.5)	50 (57.5)	0.661	36 (41.4)	51 (58.6)	0.366	30 (34.5)	57 (65.5)	0.485	15 (17.2)	72 (82.8)	0.402
Positive	27	18 (66.7)	9 (33.3)		13 (48.1)	14 (51.9)		8 (29.6)	19 (70.4)		7 (25.9)	20 (74.1)		7 (25.9)	20 (74.1)	

MI, muscle invasive; NMI, non-muscle invasive; NMIP, non-muscle invasive papillary; UC, urothelial carcinoma.
[a] χ^2 or Fisher's exact tests.

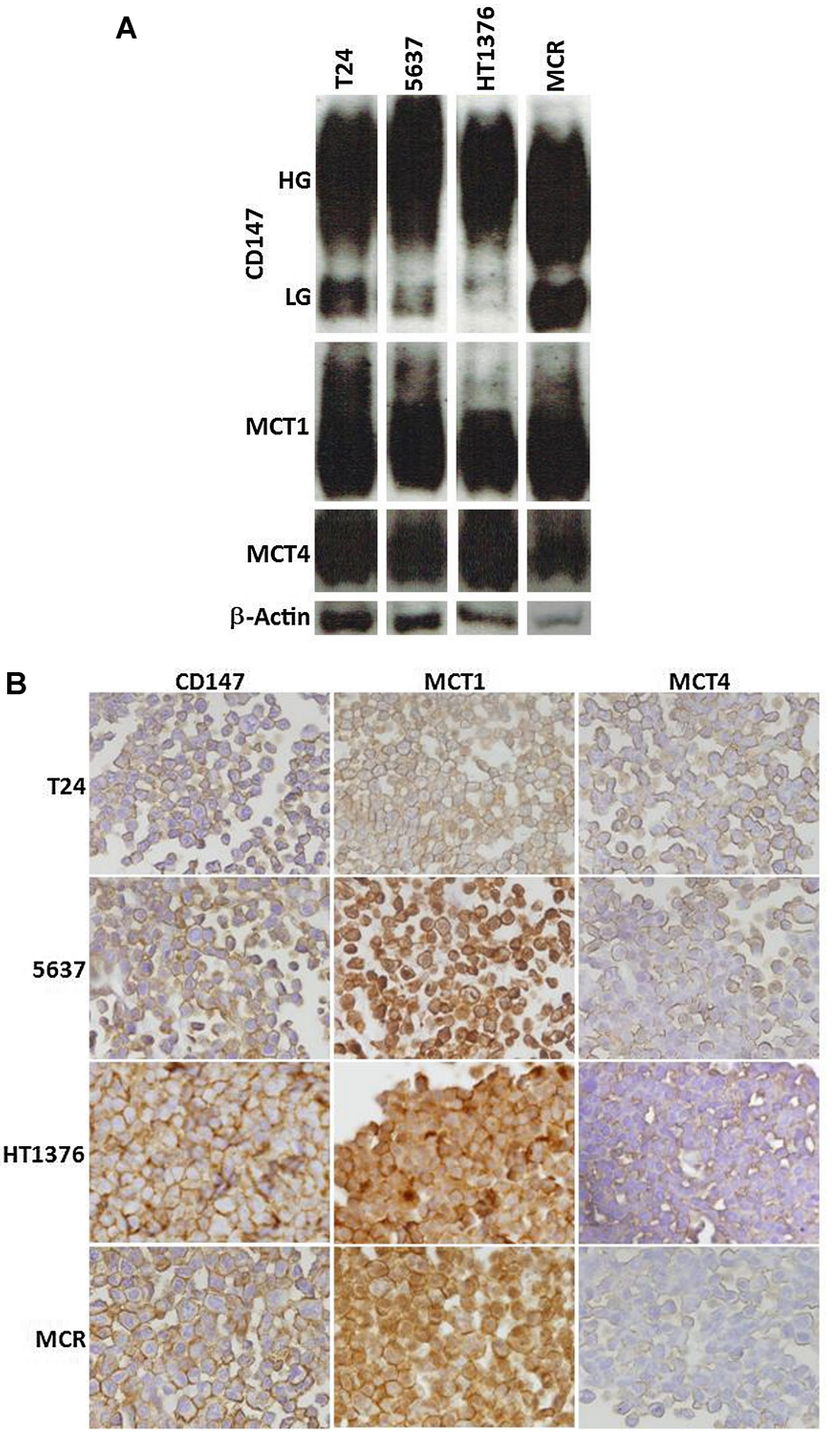

Figure 2. CD147 and monocarboxylate transporters (MCT1 and MCT4) expressions in bladder cancer cell lines, as detected by Western blot (A; molecular weights: 50–60 kDa for the highly glycosylated and 42 kDa for low glycosylated form of CD147, 50 kDa for MCT1, and 52 kDa for MCT4) and immunocytochemistry (B, ×400 amplification). The biomarkers were expressed by the four UBC cell lines. The pattern of expression was predominantly membranous. 5637, HT1376 and MCR additionally exhibited a strong cytoplasmic immunoreaction for MCT1.

(methotrexate, vinblastine, adriamycin, and cisplatin) and GC (gemcitabine and cisplatin) combinations generally used to treat MI-UBC patients [27]. This "alkylating-like" agent exerts clinical activity against several solid malignancies, namely testicular, bladder, ovarian, colorectal, lung and head, and neck cancers [28]. However, many patients are intrinsically resistant to cisplatin-based regimens, while others are initial responders but will eventually develop resistance [3].

Although poorly explored in UBC setting, the influence of the metabolic transformation events that alter the tumor microenvironment and thus mediate malignant progression and dissemination is gaining particular attention. In fact, solid malignancies are characterized by hypoxic regions and

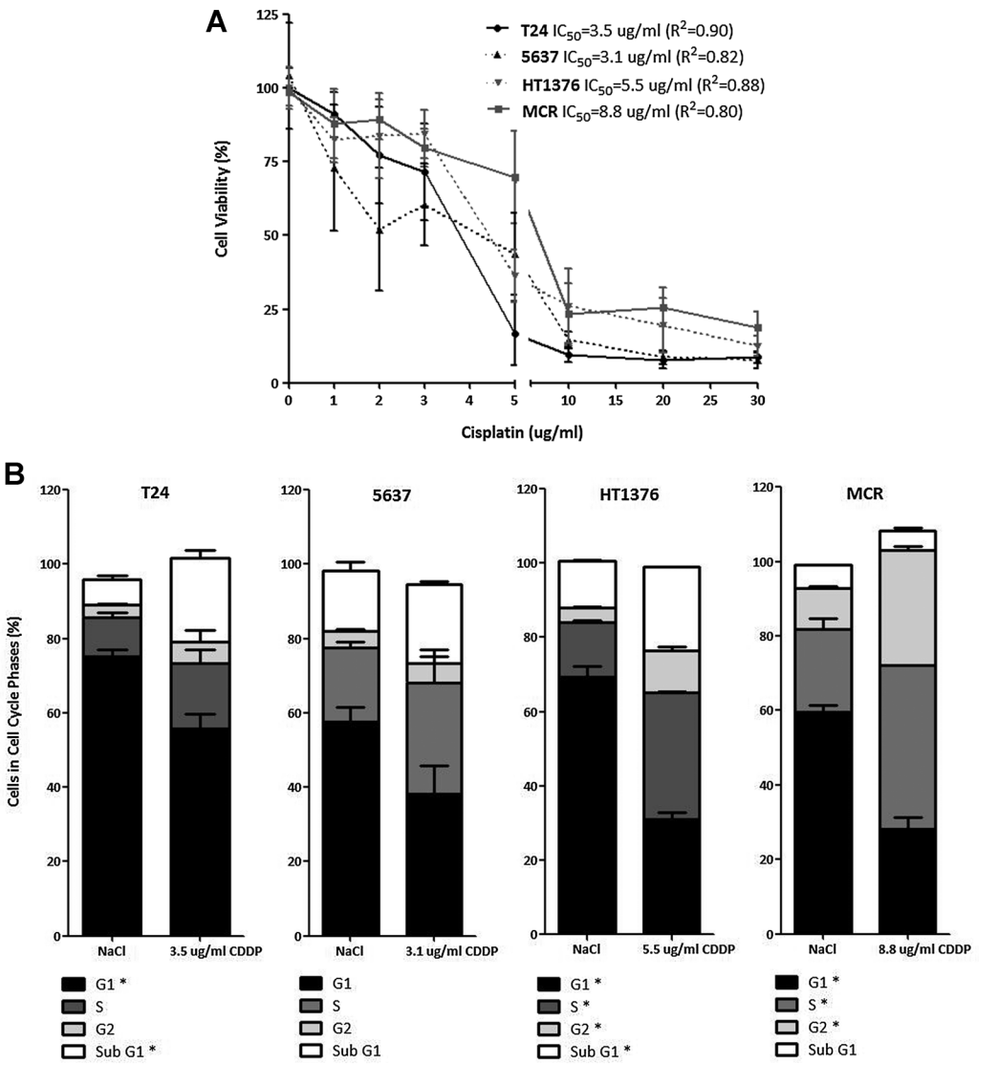

Figure 3. Effect of CDDP on the viability of bladder cancer cell lines (A), as detected by the MTS assay after 72 h of treatment. Results are expressed as the mean ± standard deviation of at least 3 independent experiments, each one in triplicate. The equation for IC_{50} determination is Y = Bottom + (To*P* − Bottom)/(1 + 10^((LogIC_{50}-X)*HillSlope)). T24 and 5637 viability was inhibited in a dose-dependent manner; HT1376 and MCR were less sensitive to CDDP effect at the initial concentrations. Cell cycle (B) and cell death (C) analysis of bladder cancer cell lines after 72 h of treatment with IC_{50} values of CDDP, as detected by the propidium iodide (PI) and the Annexin V/PI assays, respectively (flow cytometry). Results are expressed as the mean ± standard deviation of at least 3 independent experiments. $^{*}P < 0.05$, compared IC_{50} CDDP with NaCl. Representative dotplots of cell population distribution stained for Annexin V and PI are shown (cell population in bottom/left (black dots) = viable cells; cell population in upper/right = death cells (red dots, late apoptosis; green dots, necrosis)]. CDDP exerted a cytotoxic effect on T24 and 5637 cell lines, as confirmed by an increase in subG1 phase cell populations, in the cell cycle analysis, and an increase in late apoptotic/necrotic cell populations, in the cell death analysis. HT1376 and MCR cells were arrested in S phase (cell cycle analysis), and no difference was observed between control and treated conditions in the cell death analysis, which denotes a cytostatic action of CDDP.

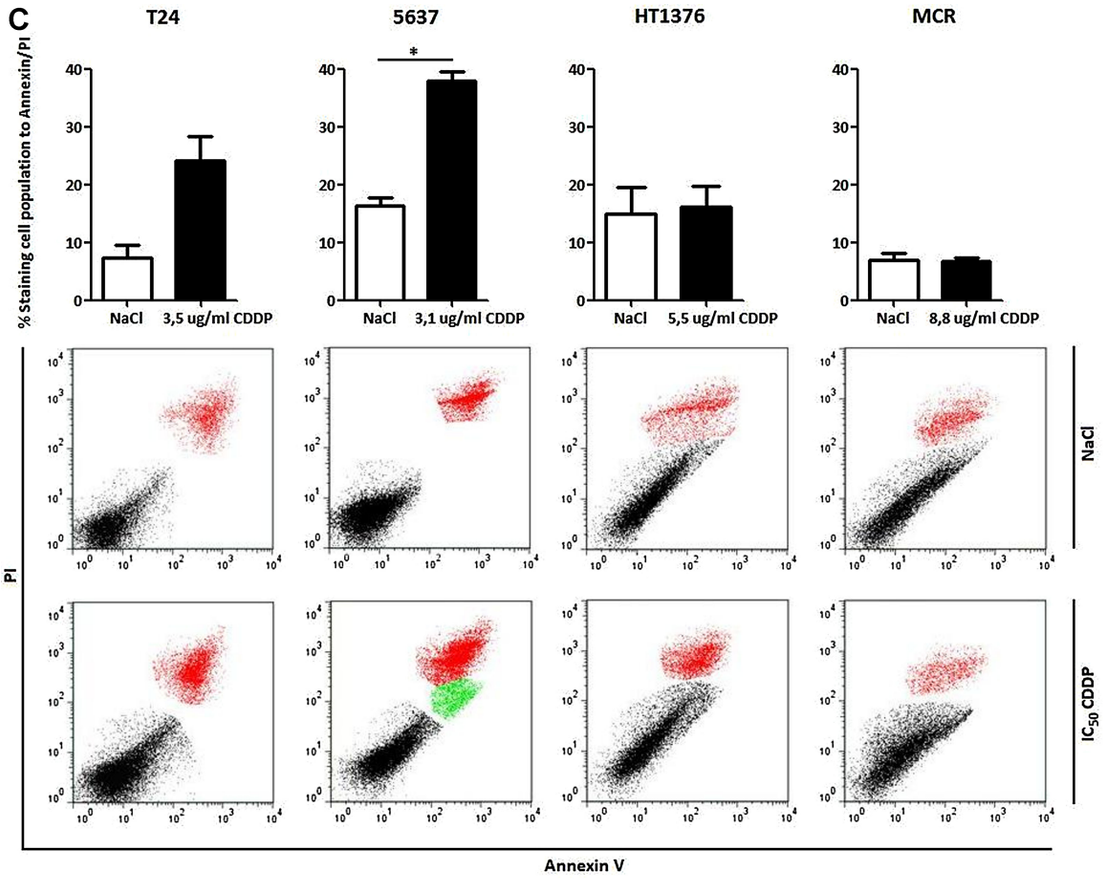

Figure 3. (*Continued*)

increased anaerobic and aerobic glycolysis, acidic-promoting conditions that facilitate metastasis and chemoresistance [29]. In order to further unravel the role of microenvironment-related molecules in bladder cancer, we initiated our study by characterizing the clinico-pathological and prognostic significance of MCT1, MCT4, CD147, CD44, and CAIX in a cohort of 114 UBC patients.

To our knowledge, this is the first study evaluating MCTs expression in bladder tumor tissue. We found a considerable percentage of tumor sections positive for MCT1 and MCT4. The malignant cells were stained in the cytoplasm and/or in the plasma membrane. The biomarkers were largely absent in the non-neoplastic sections. Plasma membrane expression was only relevant for MCT1, which probably indicates that this isoform is essential for the transport of lactate from the malignant glycolytic cells to the extracellular milieu. Additionally, the cytoplasmic expression found for both biomarkers possible denotes their accessory role in the metabolism of UBC cells, by transporting monocarboxylates, namely lactate and pyruvate, across the membranes of cellular organelles. In fact, MCT1 and MCT4 have also been localized in the mitochondrial membrane [30]. UBC patients with positive tumors, particularly for MCT1, displayed unfavorable clinico-pathological profiles. In accordance, MCTs upregulation has also been observed in other malignant contexts [17,24,31].

In vivo and in vitro studies have described CD147 has a chaperone for MCT1 and MCT4 [32,33], which was similarly supported by immunoexpression studies with human tissues [17,31]. In our UBC cohort, MCT1 and MCT4 expressions were also significantly correlated with CD147 expression. Besides its function as a chaperone, CD147 directly promotes the malignant phenotype, being upregulated in several tumor types [17,31]. We have previously demonstrated that CD147 overexpression, included in a model of UBC aggressiveness, facilitates the discrimination of bladder cancer patients' prognosis [13]. In the current study, CD147 was upregulated in bladder tumor tissue, significantly associating with tumor aggressiveness and poor prognosis. In accordance, a few studies have identified CD147 expression in UBC as an independent prognostic factor [11,12], being able to predict response to cisplatin-containing regimens [12]. In our cohort, the concurrent expression

of MCT1 and CD147 significantly associated with unfavorable clinico-pathological parameters and poor prognosis. Other studies with distinct malignancies have demonstrated that the prognostic value of CD147 is associated with its co-expression with MCT1 [34]. MCTs seem to be necessary for proper membrane expression of CD147 [35], and a cooperative role between the two types of biomarkers in determining chemotherapy resistance has been proposed [16]. Although the number of eligible cases was low, the CD147/MCT1 double-positive profile discriminated, in our UBC cohort, a poor-prognosis group within patients who received platinum-based chemotherapy. Thus, besides acting as lactate transporters and pH regulators, MCTs may also play indirect roles in angiogenesis, invasion, malignant dissemination and chemoresistance, by regulating and interacting with CD147. It has been described that CD147 enhances tumor growth and chemoresistance via the phosphatidylinositol 3-kinase (PI3K)/Akt pathway in a hyaluronan-dependent manner [36]. In fact, CD147 stimulates hyaluronan production [37]. Besides its important structural function, this ubiquitous glycosaminoglycan plays also instructive roles in signaling via binding to specific cell-surface receptors, namely CD44 [38]. CD44 is a multifunctional transmembrane glycoprotein involved in cell adhesion and migration [39]. In our study, we observed that the majority of the UBC samples expressed CD44, mainly at the plasma membrane, which was significantly correlated with tumor progression. These results are in agreement with those obtained by other authors [14,40]. Moreover, there was a substantial concordance between plasma membrane expression of MCTs and CD44, on one hand, and CD147 and CD44, on the other hand. It has been demonstrated that constitutive interactions among hyaluronan, CD44, and CD147 contribute to regulate MCTs localization and function [6]. Our results seem to support that theory. We may hypothesise that this interactive profile points out for a probable partnership between CD44, MCTs. and CD147 in regulating the hyper-glycolytic and acid-resistant phenotype, and also chemotherapy resistance. CD147 stimulates hyaluronan production [37], but lactate also induces synthesis of hyaluronan and expression of CD44 variants in stromal and

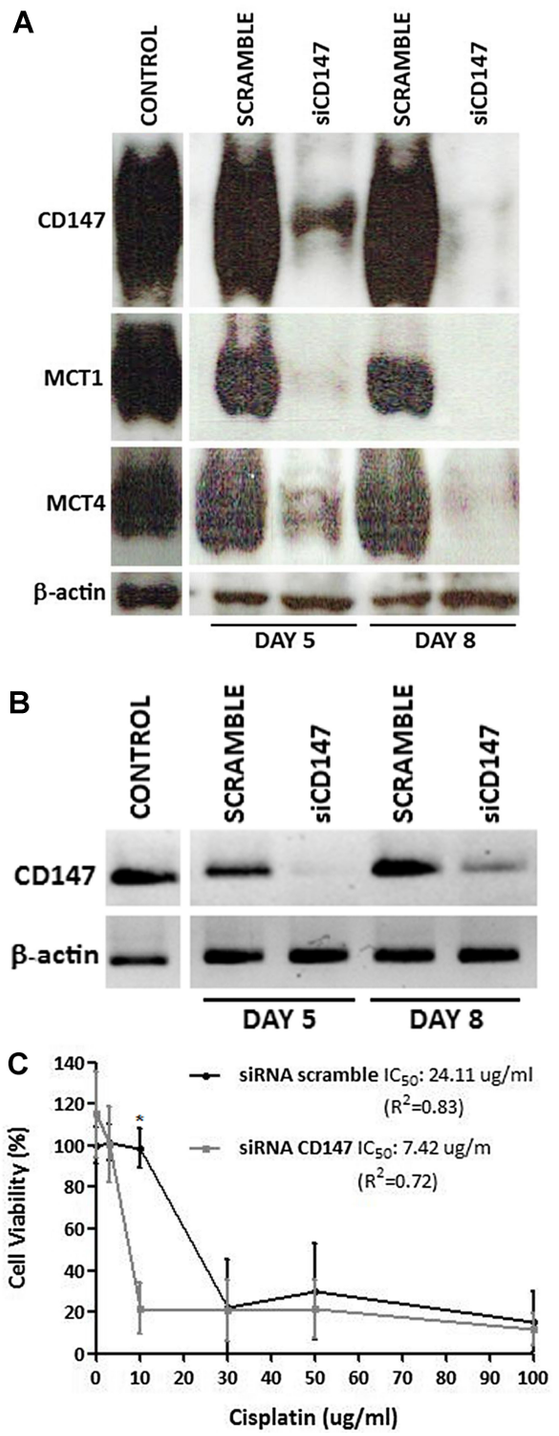

Figure 4. Effect of CD147 downregulation in HT1376 cell line on the expression of MCTs and on chemosensitivity to CDDP (treatment with CDDP between days 5 and 8 after reverse transfection). A, Western blot analysis of CD147, MCT1 and MCT4 expressions in control/scramble HT1376 cells and in siCD147 HT1376 cells showing that CD147 silencing was accompanied by a decrease in MCT1 and MCT4 expressions (molecular weights: 50–60 kDa for the highly glycosylated and 42 kDa for low glycosylated form of CD147, 50 kDa for MCT1, and 52 kDa for MCT4). B, RT-PCR analysis of CD147 expression in control/scramble HT1376 cells and in siCD147 HT1376 cells confirming its suppression at the RNA level at days 5 and 8 after reverse transfection (molecular weight of CD147: 196 bp). C, effect of CDDP on the viability of scramble and siCD147-HT1376 cells, as detected by the MTS assay after 72 h of treatment, showing that siCD147 cells were more sensitive to CDDP. Results are expressed as the mean ± standard deviation of at least 3 independent experiments, each one in triplicate. $^{*}P < 0.05$, compared IC_{50} from scramble cells with siCD147 cells. The equation for IC_{50} determination is Y = Bottom + (Top − Bottom)/(1 + 10^((LogIC_{50}-X)*HillSlope)).

tumor cells [41]. Moreover, hyaluronan-CD44 binding influences the activity of several downstream signalling pathways, namely the anti-apoptotic MAPK (mitogen-activated protein kinase) and PI3K-Akt pathways, consequently promoting tumor cell proliferation, survival, motility, invasiveness, and chemoresistance [42]. A few studies have shown that hyaluronan-CD44 signalling promotes cisplatin resistance in head and neck, and in lung cancers [43,44]. Other chemoresistance-mediating hyaluronan-dependent mechanisms have been described, namely EGFR (epidermal growth factor receptor)-mediated oncogenic signaling [45], or acquisition of cancer stem cell properties due to CD44 interaction with cancer stem cell markers and subsequent activation of microRNAs [46]. Additional studies are necessary to further clarify how cell surface interactions among hyaluronan, CD44, CD147, and MCTs contribute to initiate molecular responses that impair chemotherapy—namely cisplatin—effects.

In our immunohistochemistry study, we also evaluated CAIX expression, a catalyst that contributes to the generation of the acid-resistant phenotype under hypoxic conditions [47]. We observed that the vast majority of the UBC samples expressed this biomarker, with the luminal face of NMI papillary tumors and the tumor core in MI lesions being intensely stained. CAIX positivity was predominant in high-grade papillary tumors, and seemed to associate with a low aggressiveness profile. Several authors have also reported a higher expression of CAIX in NMI than in MI tumors [15,48], although their reports generally pointed out for an association between CAIX upregulation and occurrence of recurrence, progression and poor overall survival. In the study by Hussain et al. [48], there was a tendency towards longer survival for patients with tumors expressing CAIX strongly. Probably, in their study, as well as in our cohort, the high rate of CAIX expression in papillary lesions influenced the clinicopathological and survival data. Interestingly, significant associations were found when we compared immunoreactive samples for MCT4, CD147, and CD44 with CAIX plasma membrane positive cases. These results most likely reflect the adjustment to a hypoxia-mediated glycolytic metabolism that upregulates MCTs and their chaperones.

Our important results on the prognostic and platinum-response discriminatory significance of CD147 in UBC patients led us to further explore its biological role in an in vitro assay. We started by confirming the expression of CD147, MCT1, and MCT4 in four parental UBC cell lines. We then characterized the effect of cisplatin treatment on cell viability, cell cycle distribution and cell death. Different responses were obtained, which probably reflects the natural heterogeneity in UBC pathology, biology and response to treatment. Overall, the NMI 5637 cell line and the MI T24 cell line were the most sensitive to cisplatin treatment, as observed by the effective decrease in cell viability, the increase in S and subG1 phase cell populations, and the higher apoptotic rate. Similar results were obtained by Pinto-Leite et al. [49]. The MI HT1376 and MCR cell lines were less sensitive to cisplatin treatment, with the drug exerting a cytostatic effect on these cells, as confirmed by the higher IC_{50} value, and the cell cycle/death data. Based on these observations, we downregulated CD147 expression on MCR and HT1376 cells using the RNA interference (siRNA) approach, although we were not able to conclude the assay with MCR cells, since they did not tolerate CD147 downregulation plus cisplatin treatment. The suppression of CD147 expression in a single UBC cell line could be a limitation, together with the possible generation of false positives due to off-target effects inherent to the use of a single siRNA construct. Despite this, CD147 silencing in HT1376 cells was accompanied by a marked decrease in MCT1 and MCT4 expressions, confirming that MCTs rely on CD147 for their proper expression and function. Moreover, CD147 downregulation clearly increased chemosensitivity to cisplatin, which supports the hypothesis that this multifunctional protein mediates chemoresistance in UBC. In accordance, Wang et al. [50] and Zhu et al. [51] used a similar approach in gastric and laryngeal cell lines, and also demonstrated that suppression of CD147 expression sensitizes cells to cisplatin.

In summary, our findings indicate that microenvironment-related molecules, particularly CD147 and MCT1, are implicated in bladder cancer progression and resistance to cisplatin-based chemotherapy, unraveling new possibilities for target therapeutic intervention. Improvement of the methodological approach for obtaining cisplatin resistant UBC sublines (with an intermittent stepwise selection protocol), and additional in vitro and in vivo studies, are warranted to clarify the molecular mechanisms involved in this biological scenario.

ACKNOWLEDGMENTS

We thank Prof. Paula Videira for providing the bladder cancer cell lines, to Dr. Rosário Pinto-Leite for cell line authentication, and to the Pharmaceutical Services of the Portuguese Institute of Oncology for providing the stock solutions of cisplatin. This study was supported by the Life and Health Sciences Research Institute (ICVS) from the School of Health Sciences of the University of Minho. VM-G received a PhD fellowship from the Portuguese Science and Technology Foundation (FCT, ref. SFRH/BD/51997/2012).

REFERENCES

1. Colombel M, Soloway M, Akaza H, et al. Epidemiology, staging, grading, and risk stratification of bladder cancer. Eur Urol Suppl 2008;7:618–626.

2. Cheung G, Sahai A, Billia M, Dasgupta P, Khan MS. Recent advances in the diagnosis and treatment of bladder cancer. BMC Med 2013;11:13.
3. Galluzzi L, Senovilla L, Vitale I, et al. Molecular mechanisms of cisplatin resistance. Oncogene 2012;31:1869–1883.
4. Weidle UH, Scheuer W, Eggle D, Klostermann S, Stockinger H. Cancer-related issues of CD147. Cancer Genomics Proteomics 2010;7:157–169.
5. Toole BP, Slomiany MG. Hyaluronan, CD44 and Emmprin: Partners in cancer cell chemoresistance. Drug Resist Updat 2008;11:110–121.
6. Slomiany MG, Grass GD, Robertson AD, et al. Hyaluronan, CD44, and emmprin regulate lactate efflux and membrane localization of monocarboxylate transporters in human breast carcinoma cells. Cancer Res 2009;69:1293–1301.
7. Halestrap AP. The SLC16 gene family–Structure, role and regulation in health and disease. Mol Aspects Med 2013; 34:337–349.
8. Upadhyay M, Samal J, Kandpal M, Singh OV, Vivekanandan P. The Warburg effect: Insights from the past decade. Pharmacol Ther 2013;137:318–330.
9. Gillies RJ, Gatenby RA. Adaptive landscapes and emergent phenotypes: Why do cancers have high glycolysis? J Bioenerg Biomembr 2007;39:251–257.
10. Brahimi-Horn MC, Bellot G, Pouyssegur J. Hypoxia and energetic tumour metabolism. Curr Opin Genet Dev 2011; 21:67–72.
11. Xue YJ, Lu Q, Sun ZX. CD147 overexpression is a prognostic factor and a potential therapeutic target in bladder cancer. Med Oncol 2011;28:1363–1372.
12. Als AB, Dyrskjot L, von der Maase H, et al. Emmprin and survivin predict response and survival following cisplatin-containing chemotherapy in patients with advanced bladder cancer. Clin Cancer Res 2007;13:4407–4414.
13. Afonso J, Longatto-Filho A, Baltazar F, et al. CD147 over-expression allows an accurate discrimination of bladder cancer patients' prognosis. Eur J Surg Oncol 2011;37:811–817.
14. Omran OM, Ata HS. CD44s and CD44v6 in diagnosis and prognosis of human bladder cancer. Ultrastruct Pathol 2012; 36:145–152.
15. Klatte T, Seligson DB, Rao JY, et al. Carbonic anhydrase IX in bladder cancer: A diagnostic, prognostic, and therapeutic molecular marker. Cancer 2009;115:1448–1458.
16. Takata R, Katagiri T, Kanehira M, et al. Predicting response to methotrexate, vinblastine, doxorubicin, and cisplatin neoadjuvant chemotherapy for bladder cancers through genome-wide gene expression profiling. Clin Cancer Res 2005;11: 2625–2636.
17. Pinheiro C, Longatto-Filho A, Azevedo-Silva J, Casal M, Schmitt FC, Baltazar F. Role of monocarboxylate transporters in human cancers: State of the art. J Bioenerg Biomembr 2012;44:127–139.
18. Negi LM, Talegaonkar S, Jaggi M, Ahmad FJ, Iqbal Z, Khar RK. Role of CD44 in tumour progression and strategies for targeting. J Drug Target 2012;20:561–573.
19. Supuran CT. Inhibition of carbonic anhydrase IX as a novel anticancer mechanism. World J Clin Oncol 2012;3:98–103.
20. Amin MB, Srigley JR, Grignon DJ, et al. Urinary bladder cancer protocols and checklists. Northfield: College of American Pathologists 2005.
21. Edge SB, Byrd DR, Compton CC, Fritz AG, Greene FL, Trotti A. AJCC Cancer Staging Manual. New York: Springer Verlag; 2010.
22. Eble JN, Sauter G, Epstein JI, Sesterhenn IA. Pathology and Genetics of Tumours of the Urinary System and Male Genital Organs. Lyon: IARC Press 2004.
23. Pinto-Leite R, Carreira I, Melo J, et al. Genomic characterization of three urinary bladder cancer cell lines: Understanding genomic types of urinary bladder cancer. Tumour Biol 2014.
24. Pinheiro C, Reis RM, Ricardo S, Longatto-Filho A, Schmitt F, Baltazar F. Expression of monocarboxylate transporters 1, 2 and 4 in human tumours and their association with CD147 and CD44. J Biomed Biotechnol 2010;2010:427694.
25. Pinheiro C, Sousa B, Albergaria A, et al. GLUT1 and CAIX expression profiles in breast cancer correlate with adverse prognostic factors and MCT1 overexpression. Histol Histopathol 2011;26:1279–1286.
26. Pertega-Gomes N, Vizcaino JR, Miranda-Goncalves V, et al. Monocarboxylate transporter 4 (MCT4) and CD147 overexpression is associated with poor prognosis in prostate cancer. BMC Cancer 2011;11:312.
27. Sternberg CN, Bellmunt J, Sonpavde G, et al. ICUD-EAU International Consultation on Bladder Cancer 2012: Chemotherapy for urothelial carcinoma-neoadjuvant and adjuvant settings. Eur Urol 2013;63:58–66.
28. Harper BW, Krause-Heuer AM, Grant MP, Manohar M, Garbutcheon-Singh KB, Aldrich-Wright JR. Advances in platinum chemotherapeutics. Chemistry 2010;16:7064–7077.
29. Schiavoni G, Gabriele L, Mattei F. The tumor microenvironment: A pitch for multiple players. Front Oncol 2013;3:90.
30. Benton CR, Campbell SE, Tonouchi M, Hatta H, Bonen A. Monocarboxylate transporters in subsarcolemmal and intermyofibrillar mitochondria. Biochem Biophys Res Commun 2004;323:249–253.
31. Miranda-Goncalves V, Honavar M, Pinheiro C, et al. Monocarboxylate transporters (MCTs) in gliomas: Expression and exploitation as therapeutic targets. Neuro Oncol 2013;15: 172–188.
32. Wilson MC, Meredith D, Fox JE, Manoharan C, Davies AJ, Halestrap AP. Basigin (CD147) is the target for organomercurial inhibition of monocarboxylate transporter isoforms 1 and 4: The ancillary protein for the insensitive MCT2 is EMBIGIN (gp70). J Biol Chem 2005;280:27213–27221.
33. Kirk P, Wilson MC, Heddle C, Brown MH, Barclay AN, Halestrap AP. CD147 is tightly associated with lactate transporters MCT1 and MCT4 and facilitates their cell surface expression. EMBO J 2000;19:3896–3904.
34. Pinheiro C, Longatto-Filho A, Simoes K, et al. The prognostic value of CD147/EMMPRIN is associated with monocarboxylate transporter 1 co-expression in gastric cancer. Eur J Cancer 2009;45:2418–2424.
35. Gallagher SM, Castorino JJ, Wang D, Philp NJ. Monocarboxylate transporter 4 regulates maturation and trafficking of CD147 to the plasma membrane in the metastatic breast cancer cell line MDA-MB-231. Cancer Res 2007;67:4182–4189.
36. Misra S, Ghatak S, Zoltan-Jones A, Toole BP. Regulation of multidrug resistance in cancer cells by hyaluronan. J Biol Chem 2003;278:25285–25288.
37. Marieb EA, Zoltan-Jones A, Li R, et al. Emmprin promotes anchorage-independent growth in human mammary carcinoma cells by stimulating hyaluronan production. Cancer Res 2004;64:1229–1232.
38. Toole BP. Hyaluronan: From extracellular glue to pericellular cue. Nat Rev Cancer 2004;4:528–539.
39. Ponta H, Sherman L, Herrlich PA. CD44: From adhesion molecules to signalling regulators. Nat Rev Mol Cell Biol 2003;4:33–45.
40. Kramer MW, Escudero DO, Lokeshwar SD, et al. Association of hyaluronic acid family members (HAS1, HAS2, and HYAL-1) with bladder cancer diagnosis and prognosis. Cancer 2011; 117:1197–1209.
41. Rudrabhatla SR, Mahaffey CL, Mummert ME. Tumor microenvironment modulates hyaluronan expression: The lactate effect. J Invest Dermatol 2006;126:1378–1387.
42. Toole BP. Hyaluronan-CD44 Interactions in Cancer: Paradoxes and Possibilities. Clin Cancer Res 2009;15:7462–7468.
43. Ohashi R, Takahashi F, Cui R, et al. Interaction between CD44 and hyaluronate induces chemoresistance in non-small cell lung cancer cell. Cancer Lett 2007;252:225–234.
44. Torre C, Wang SJ, Xia W, Bourguignon LY. Reduction of hyaluronan-CD44-mediated growth, migration, and cisplatin

resistance in head and neck cancer due to inhibition of Rho kinase and PI-3 kinase signaling. Arch Otolaryngol Head Neck Surg 2010;136:493–501.
45. Wang SJ, Bourguignon LY. Hyaluronan and the interaction between CD44 and epidermal growth factor receptor in oncogenic signaling and chemotherapy resistance in head and neck cancer. Arch Otolaryngol Head Neck Surg 2006;132: 771–778.
46. Bourguignon LY, Wong G, Earle C, Chen L. Hyaluronan-CD44v3 interaction with Oct4-Sox2-Nanog promotes miR-302 expression leading to self-renewal, clonal formation, and cisplatin resistance in cancer stem cells from head and neck squamous cell carcinoma. J Biol Chem 2012;287:32800–32824.
47. Swietach P, Vaughan-Jones RD, Harris AL. Regulation of tumor pH and the role of carbonic anhydrase 9. Cancer Metastasis Rev 2007;26:299–310.
48. Hussain SA, Palmer DH, Ganesan R, et al. Carbonic anhydrase IX, a marker of hypoxia: Correlation with clinical outcome in transitional cell carcinoma of the bladder. Oncol Rep 2004; 11:1005–1010.
49. Pinto-Leite R, Arantes-Rodrigues R, Palmeira C, et al. Everolimus combined with cisplatin has a potential role in treatment of urothelial bladder cancer. Biomed Pharmacother 2013;67:116–121.
50. Wang B, Xu YF, He BS, et al. RNAi-mediated silencing of CD147 inhibits tumor cell proliferation, invasion and increases chemosensitivity to cisplatin in SGC7901 cells in vitro. J Exp Clin Cancer Res 2010;29:61.
51. Zhu C, Pan Y, He B, et al. Inhibition of CD147 gene expression via RNA interference reduces tumor cell invasion, tumorigenicity and increases chemosensitivity to cisplatin in laryngeal carcinoma Hep2 cells. Oncol Rep 2011;25:425–432.